Characteristics of Turbulence and Dispersion of Pollutants Near Major Highways

S. TRIVIKRAMA RAO AND LEON SEDEFIAN

Division of Air Resources, New York State Department of Environmental Conservation, Albany 12233

ULRICH H. CZAPSKI

Department of Atmospheric Science, State University of New York at Albany, Albany 12222

(Manuscript received 13 May 1978, in final form 16 September 1978)

ABSTRACT

The primary objective of this study is to assess the effect of traffic on the turbulence structure and to infer the time and space scales of the eddies generated by the traffic. To this end, time series of wind and temperature were obtained by a three-component sonic anemometer and by copper-constantan thermocouples adjacent to the Long Island Expressway in New York State. Eddy fluxes of heat and momentum were computed under different atmospheric conditions. Spectral distributions of these parameters were obtained using the fast Fourier transform technique. The flow characteristics in the surface layer are inferred from the wind profiles adjacent to the highway.

Results show a distinct bulge in the high-frequency range of the wind spectrum. This bulge appears only during moderate to heavy traffic conditions and with wind across the highway. This traffic-induced turbulent energy appears to be dominant at mean frequencies to 0.1–1.0 Hz corresponding to eddy sizes of the order of a few meters. Even under quite stable atmospheric conditions, no organized convection due to vehicle exhaust heat can be distinguished in the spectral structure. The aerodynamic drag due to the moving vehicles on the highway is manifested by a pronounced acceleration of wind in the lowest 8 m, especially in the cases of wind directions nearly parallel to the highway. The impact of traffic-induced turbulence on the near-roadway dispersion of air pollutants is also discussed.

1. Introduction

Mathematical dispersion models are being widely used to estimate the pollutant concentrations adjacent to highways. Due to incomplete understanding of dispersion at the microscale, and to mathematical expediency, various assumptions and simplifications are made in the formulation of the problem. It is well known that the microscale structure of atmospheric motions over a homogeneous underlying surface are describable by similarity theories. However, mechanical turbulence generated by the moving vehicles, change in surface roughness and, perhaps, thermal input from automobile exhaust complicate the flow. In addition, aerodynamic drag along the direction of the moving traffic could have a significant effect on the surface layer structure. Significant deviations from the similarity laws could occur under the above conditions.

While there have been a number of theoretical and experimental studies of flow over homogeneous surfaces, there have been only a few field studies under the complex situations outlined above. Simple changes in roughness and temperature field have been theoretically investigated by Haung and Nickerson (1974a,b), Byutner (1974) and Lo (1977), whereas field studies have been published by Stearns and Lettau (1963), Bradley (1968), Czapski and Mumford (1975), Munro and Oke (1975), Jackson (1976) and Peterson *et al.* (1976). These studies indicate that a shallow internal boundary layer is formed, within which the wind profile is somewhat distorted from its logarithmic shape. Further, spectra and cospectra over inhomogeneous terrain (Busch and Panofsky, 1968; Fichtl and McVehil, 1970) show no distinct deviation from the inertial subrange laws.

In order to assess the weaknesses of and to suggest improvements to the mathematical dispersion models, a comprehensive data acquisition program was undertaken by the New York State Department of Environmental Conservation (see Rao *et al.*, 1978a), at a selected location of the Long Island Expressway (I-495). As a part of this major investigation special micrometeorological measurements were made in cooperation with the State University of New York at Albany. The major emphasis of this microscale study was on the evaluation of the influence of the traffic on the turbulent structure of the surface layer. Special attention was given to identification of the

0021-8952/79/030283-11$06.75

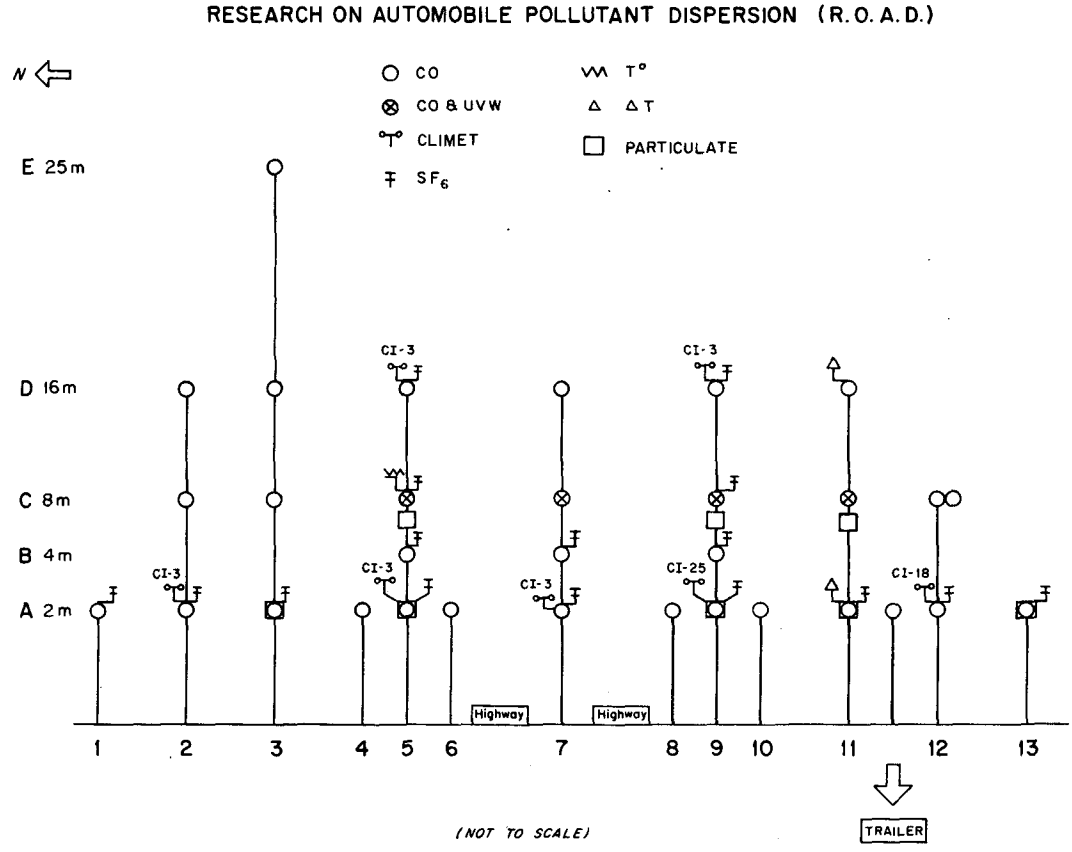

FIG. 1. Tower configuration across highway.

effects of local turbulence sources on the dispersion of pollutants.

In this paper, spectra and cospectra of the wind components and temperature for various combinations of atmospheric stability conditions, traffic volume and wind orientation with respect to the highway are presented. Also, surface layer structure is inferred from the shape of the wind profiles both upwind and downwind from the highway. Further, the effect of the local source of turbulence on the pollutant concentration (tracer gas) profiles is discussed. The features observed at the site are compared with the theoretical predictions. Deviations from theory are interpreted and their impact on near-roadway dispersion is discussed.

2. Experimental set-up and data acquisition techniques

a. Description of site

The site selected for the study was a heavily traveled straight segment of the Long Island Expressway of suburban New York. The northern and southern side of the highway are clear of buildings. A large sod farm is situated to the north and small brush is on the south side. The expressway runs approximately east–west ~2 m below the surrounding terrain.

b. Location of instruments

Seven towers were erected in a plane perpendicular to the highway. Locations of various meteorological and air quality measuring sensors in the main project are shown in Fig. 1. A three-component sonic anemometer was mounted for selected periods of time on towers 2, 9 and 11 at a height of 3 m on a 3 m extension arm. Temperature fluctuations were measured by ultra-fast copper-constantan thermocouples at approximately the center of the sonic antenna. Two wind profiler systems were located on extension arms (1 m away from the tower) at heights of 1.5, 2, 3, 5, 8 and 11 m on tower 9 and 2, 3, 5 and 8 m on tower 3.

c. Data acquisition and reduction

The constructional and operational detail of the sonic anemometer (Kaijo Denki Ltd. Model 311) has been described repeatedly in the literature (see Japan–U.S. Joint Study Group Report, 1971). The same procedures as in previous studies (Kaimal *et al.*, 1968; Czapski and Mumford, 1975) were followed. In particular, corrections for overestimation and zero drift inherent in our instrument were incorporated into the data reduction routine. The signals as well as the output of the Honeywell Accudata amplifier for the

TABLE 1. Summary of the experimental conditions for the sonic anemometer runs. $\bar{U}$ is the mean horizontal wind speed and $\bar{W}$ the mean vertical wind speed. TET and TWT are the total number of vehicles in the eastbound and westbound directions, respectively. σ_u and σ_w are the standard deviations of the along-wind and vertical component of wind velocity. $\overline{uw}$ and $\overline{wT}$ are the stress and heat flux averaged over the sampling period.

Run no.	Date	Time of the run	Wind direction	Stability	$\bar{U}$ (cm s^{-1})	$\bar{W}$ (cm s^{-1})	TET
1	9/24/76	4:30 pm	320°	Unstable	162	−0.3	1250
2	9/25/76	3:00 pm	155°	Unstable	217	−5.5	1000
3	10/05/76	3:30 am	60°	Stable	226	16.0	160
4	10/05/76	7:00 pm	30°	Neutral	306	−4.8	894
5	10/06/76	12:30 am	60°	Neutral	343	−3.6	320
6	10/06/76	4:30 pm	150°	Neutral	163	2.9	1321
7	10/08/76	9:30 am	180°	Neutral	329	27.6	607
8	5/25/77	2:30 pm	295°	Neutral	358	19.2	800
9	5/26/77	2:30 am	350°	Stable	332	17.1	320
10	6/04/77	12:15 am	350°	Stable	190	33.0	660
11	6/04/77	2:00 am	320°	Stable	176	38.0	520
12	11/17/76	1:00 pm	215°	Neutral	232	8.8	628
13	11/17/76	3:30 pm	215°	Neutral	289	15.6	1206
14	11/17/76	7:00 pm	180°	Neutral	122	−5.5	893
15	11/18/76	3:30 pm	285°	Neutral	619	33.3	1226
16	11/18/76	9:15 pm	285°	Stable	255	11.2	620
17	11/19/76	10:15 am	290°	Neutral	471	21.5	518
18	10/08/76	4:15 pm	195°	Neutral	270	−8.7	1241
19	10/20/76	12:30 pm	155°	Neutral	135	6.0	532
20	10/21/76	10:45 am	300°	Neutral	664	26.0	565
21	10/21/76	3:15 pm	350°	Neutral	493	31.0	1191
22	10/22/76	7:30 pm	260°	Stable	193	−19.2	899

Run no.	Average speed of the vehicles (km h^{-1})	TWT	Average speed of the vehicles (km h^{-1})	Data from tower	σ_u (cm s^{-1})	σ_w (cm s^{-1})	$-\overline{uw}$ (cm^2 s^{-2})	$\overline{wT}$ (°C m s^{-1})
1	56.4	850	77.3	9	93.7	55.0	303	0.63
2	64.4	800	80.5	9	107.6	52.0	945	0.40
3	88.5	80	93.4	9	103.0	43.5	543	—
4	66.3	480	78.1	9	65.1	58.4	449	—
5	69.2	102	77.6	9	63.8	49.4	272	—
6	51.5	825	77.3	9	57.6	29.6	843	—
7	73.6	933	76.5	9	162.2	85.5	3695	—
8	71.6	630	75.7	9	118.9	79.7	3451	—
9	85.3	138	94.2	9	77.2	48.7	897	—
10	76.5	353	79.9	9	69.3	76.9	1319	−0.25
11	86.9	236	78.2	9	53.2	55.0	1131	−0.34
12	72.8	564	76.5	2	77.7	46.7	872	0.23
13	63.6	883	75.2	2	92.9	51.2	1078	0.49
14	71.3	440	78.9	2	40.2	25.6	316	−0.03
15	65.7	821	76.2	2	161.4	49.8	1135	0.33
16	78.1	332	78.4	2	122.6	24.7	328	−0.57
17	77.3	727	78.2	2	143.2	54.8	616	—
18	43.5	404	76.0	11	150.9	26.3	490	—
19	69.7	548	76.5	11	78.8	44.8	1165	−0.14
20	74.1	646	76.3	11	176.1	107.5	2120	0.38
21	69.2	802	77.3	11	161.0	97.6	2698	0.47
22	71.2	498	78.2	11	69.3	39.4	517	0.26

thermocouple temperature fluctuations were recorded on a Honeywell Model 5600 recorder. This recorder, in a 14-channel frequency modulated version, has ample frequency response with a 10 to 1 signal to noise ratio. A zero reference voltage was recorded with each run to provide a reference check in the playback mode.

The antenna head of the sonic anemometer was oriented for each run such that the mean wind was centered between the two horizontal pulse paths.

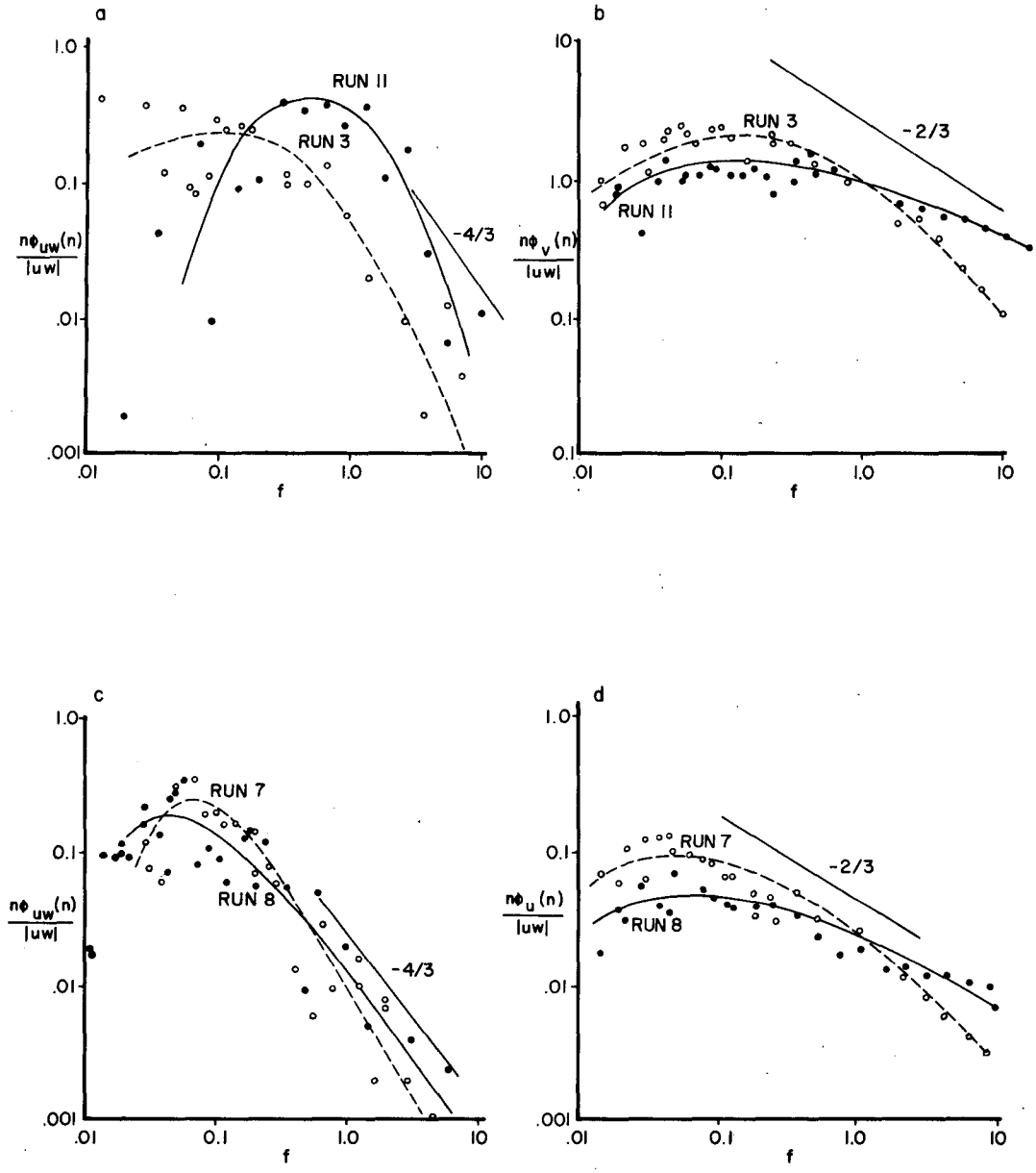

FIG. 2. (a) Normalized cospectra between along-wind (u) and vertical wind (w) components for runs 3 and 11 (stable atmospheric conditions). f is the nondimensional frequency defined as $f=nz/\bar{U}$, where n is the dimensional frequency, z the height of the measurement and $\bar{U}$ the mean wind speed. Run 11 in a case of high traffic compared to run 3. (b) Normalized spectra for the cross-wind (v) component. (c) Normalized cospectra between u and w components for runs 7 and 8 (neutral atmospheric conditions). Run 8 is a case of advection from the highway while run 7 is not. (d) Normalized spectra for the along wind (u) component.

A total of 36 h runs were obtained with as many different variations of wind direction, atmospheric stability and traffic speed and volume as possible. Each hourly run was broken into four 15 min segments to be used for processing.

The wind profiler systems, manufactured by the Thornthwaite Associates, are equipped with counters for six levels. There was also provision for automatic recording by Polaroid camera at 15 min time intervals for total times up to 12 h.

Analog records of three wind components (u,v,w) and temperature (T) were digitized by a Hewlett-Packard digital data acquisition system at a sampling rate of 20 readings/second and processed according to the procedures outlined in Czapski and Mumford (1975). Spectra of the three wind components and temperature, and cospectra of uw and wT were computed using the fast Fourier transform technique described by Rao and Ketchum (1975). No corrections for line-averaging (see Kaimal *et al.*, 1968) were made

for these spectra since inspection of the computer plots showed little effect in the frequency ranges of interest. Tilt errors and errors due to mean vertical motion were removed, however, following the method given by Hyson *et al.* (1977).

Wind profiles were determined by averaging over at least seven consecutive 15 min averages of wind speed at each level. Uniformity of data was ascertained by checking that deviations between individual 15 min samples were paralleled by similar changes at other levels. Also, comparison among wind profiles from different runs under similar conditions of wind direction, stability and traffic volume were made to ensure the consistency of data.

3. Results and discussion

a. Spectra and cospectra

Of the 36 runs of three component wind fluctuations analyzed, 22 were selected as representative of different conditions. The fluctuation statistics along with pertinent information on atmospheric stability, traffic speed and volume, wind speed and direction are presented in Table 1. The wind orientations tabulated are given with respect to the highway (0° and 180° represent perpendicular wind to the road, while 90° and 270° represent parallel wind to the road). Three stability classes are used to describe the atmospheric conditions. These were obtained from the measurements of cloud cover, wind speed, radiation and temperature differences recorded at the site.

Selected spectra and cospectra showing the influence of traffic are presented in Fig. 2. Fig. 2a presents the cospectrum for uw, representing the turbulent transport of momentum or shearing stress, for runs 3 and 11 (both cases are with advection from the highway toward the instrument), where run 11 is a case of relatively high traffic compared to run 3. Both runs are taken in the early morning hours under quite stable atmospheric conditions. Fig. 2b is the spectrum of cross wind fluctuation v for the same two runs. The uw cospectrum for runs 7 and 8 are presented in Fig. 2c. In this case, run 8 is a situation with advection from the highway toward the instrument whereas run 7 is not. The spectra of the u component, for runs 7 and 8, are shown in Fig. 2d. Inspection of these spectra reveals a striking augmentation of high-frequency portion of the variance for the situations where the wind flow has been over relatively high and fast moving traffic. According to theoretical predictions and observations of surface layer turbulence (Kaimal *et al.*, 1972) and experimental studies of surface anomaly (Czapski and Mumford, 1975), the maximum spectral power should occur at lower frequencies, when stability is decreased, which is also quite evident in our results. However, the high-frequency part of all spectra should nearly coincide under proper nondimensionalization. Moreover, in conditions of equilibrium between turbulent kinetic energy production by Reynolds stresses and dissipation by viscous forces, an extended range of the spectrum should conform to the laws of inertial subrange. The fall-off rates of spectral power for the inertial subrange, transformed to $-\frac{2}{3}$ for the spectra and $-\frac{4}{3}$ for the cospectra when the abscissa is nondimensionalized as $f=nz/\bar{U}$ and the ordinate as $n\phi(n)/$ variance, are drawn in the diagrams.

In order to isolate the contribution of the moving traffic to the turbulent energy, spectra with and without traffic influence are compared under otherwise similar atmospheric conditions. The traffic-induced turbulence spectra can be derived by subtracting the dimensional energy spectrum for run 2 from run 1. Both runs 1 and 2 have similar ambient atmospheric conditions except that run 1 has traffic influence superimposed on the ambient atmosphere. The spectral differences for all the three components of wind velocity for unstable atmospheric conditions are presented in Figs. 3a–3c. Here the $\Delta\phi(n)$, the difference in the energy of each wind component, is plotted against the actual frequency n. It is interesting to see that all the three spectral differences exhibit a log-normal shape with a maximum difference around 0.25 Hz. For the stable case, the difference spectra for runs 3 and 11 (see Fig. 3d–3f) also show a log-normal type distribution. Again, under neutral atmospheric conditions, the difference spectra were found to be log-normal. A log-normal behavior suggests that the traffic-induced eddies are distributed over a wide size range. This probably is due to the breakup of the larger eddies, introduced by the traffic at frequencies near 0.25 Hz, into smaller size eddies. The range of frequencies affected by the traffic seems to be 0.1–1.0 Hz.

The difference in the spectral power of vertical component of wind is considerably lower in the unstable case compared to the stable case (see Figs. 3c,f). This suggests that the energy input of the traffic-induced turbulence is more significant under stable atmospheric conditions. The interactions across the spectrum of vertical motions induced by buoyancy (larger scale) with motions induced by the local sources could account for the observed predominance of energy in the higher frequencies under stable situation. In non-isotropic turbulence, such interactions are likely to affect a transfer of energy to the larger scales. In the stable case, however, under near isotropic conditions, interactions between motions of similar frequencies could occur. These can lead to a constructive type of interference, thereby producing the observed broad peak in Fig. 3f.

Fig. 4 presents the temperature and vertical velocity spectra for two selected situations. Run 2 represents an unstable situation with no advection from the highway, whereas run 10 is a stable situation with advection from the highway. We see quite distinctly

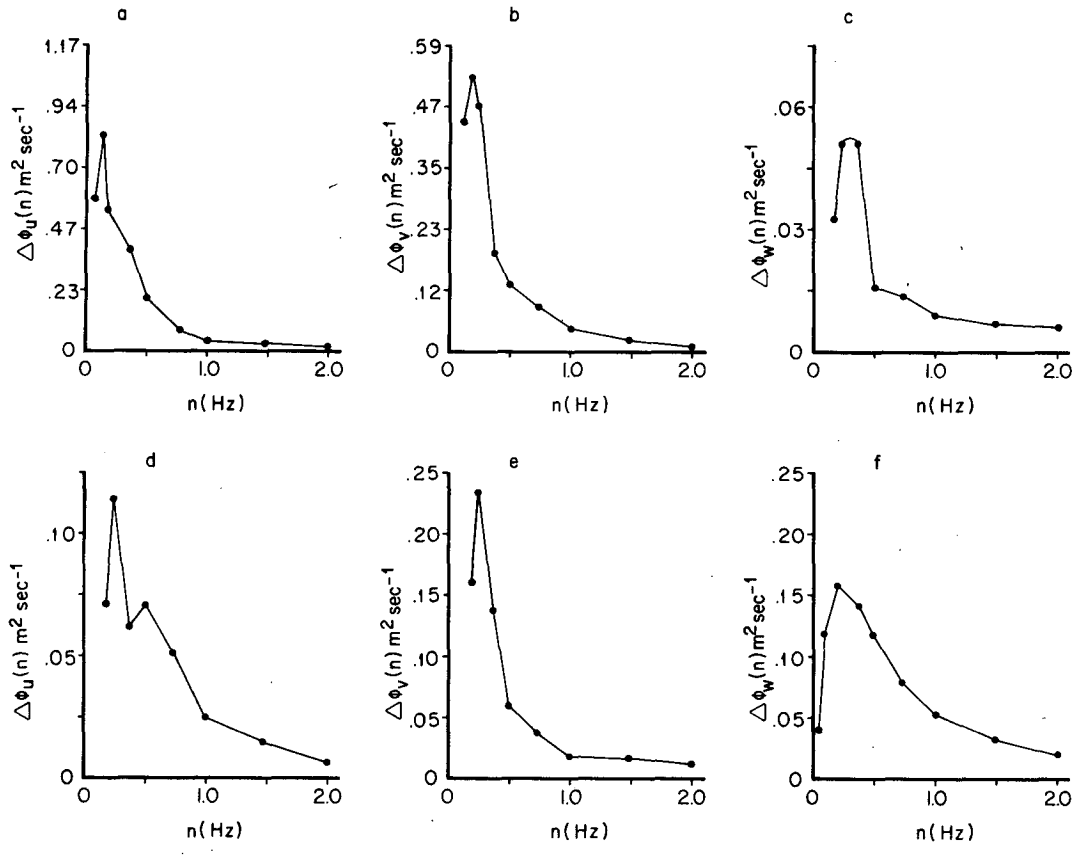

FIG. 3. (a)–(c) Difference spectra for u, v and w components, respectively, between unstable runs 1 and 2. (d)–(f) Difference spectra for u, v and w components, respectively, between stable case runs 11 and 3.

the influence of stability on the frequency of maximum spectral power (Fig. 4a against Fig. 4d), namely, a shift by one order of magnitude. While the temperature spectrum for run 2 (Fig. 4b) conforms to $-\frac{2}{3}$ law, it is interesting to see that the temperature spectrum for run 10 (Fig. 4e) significantly deviates from the $-\frac{2}{3}$ relationship. This may be attributed to the traffic-induced turbulence. The covariance between T and w is well organized in the unstable situation (Fig. 4c) compared to the stable case (Fig. 4f). Moreover, the heat flux is downward in the stable situation (see Table 1, run 10) and upward in the unstable situation, as one would expect from the natural temperature gradients.

If there were significant heat input from the automobile exhaust to induce buoyancy, one would expect to observe upward heat flux in any spectral range corresponding to the convective motions. The heat and momentum fluxes are shown together in a semi-log representation for the stable atmospheric conditions in Fig. 5. The overall heat flux for run 11 (representative of stable conditions in Fig. 5a) is downward as mentioned before. To enable the reader to see how the cospectrum of a situation with well-defined convective elements looks like, this cospectrum is compared to the cospectrum obtained over a heated water plume in Lake Ontario (see Fig. 5b), taken from Czapski and Mumford (1975), when the general conditions over the lake were stable. Examination of Fig. 5b reveals close correspondence of both wT and uw cospectra. In particular, one can readily see that at a given frequency, each positive peak in the wT cospectrum is associated with a negative peak in the uw cospectrum. The implication of this feature is that the same scales, and therefore the same mechanisms, are simultaneously transporting momentum and heat. This indicates the existence of organized convection which occurs at rather well-defined frequencies. Lack of such organization in Fig. 5a suggests that there are no significant convective motions induced by the traffic under stable atmospheric conditions. It appears that any heat input from the automobile exhaust is quickly destroyed by the mechanical turbulence generated by the moving traffic.

b. Wind profiles

Only simultaneous measurements of wind profiles on both sides of the highway are presented. The wind profiles for all the eleven cases are shown in Figure 6. Table 2 summarizes the profile data. In column 4 of Table 2 one can see that the wind direction on tower 9

at 2 m height varies only between 270 and 330°, whereas at 15 m the variation is 265 and 75°. This is obviously due to the channeling effect induced by the moving traffic and the highway configuration.

The most striking effect of the traffic on the wind profiles is the aerodynamic drag of the moving vehicles, and this feature is evident in a comparison of the profiles from tower 9 (1.5 m from the southern edge of the road) with those from tower 3 at a distance of 37 m to the north side of the highway. Runs 4, 5

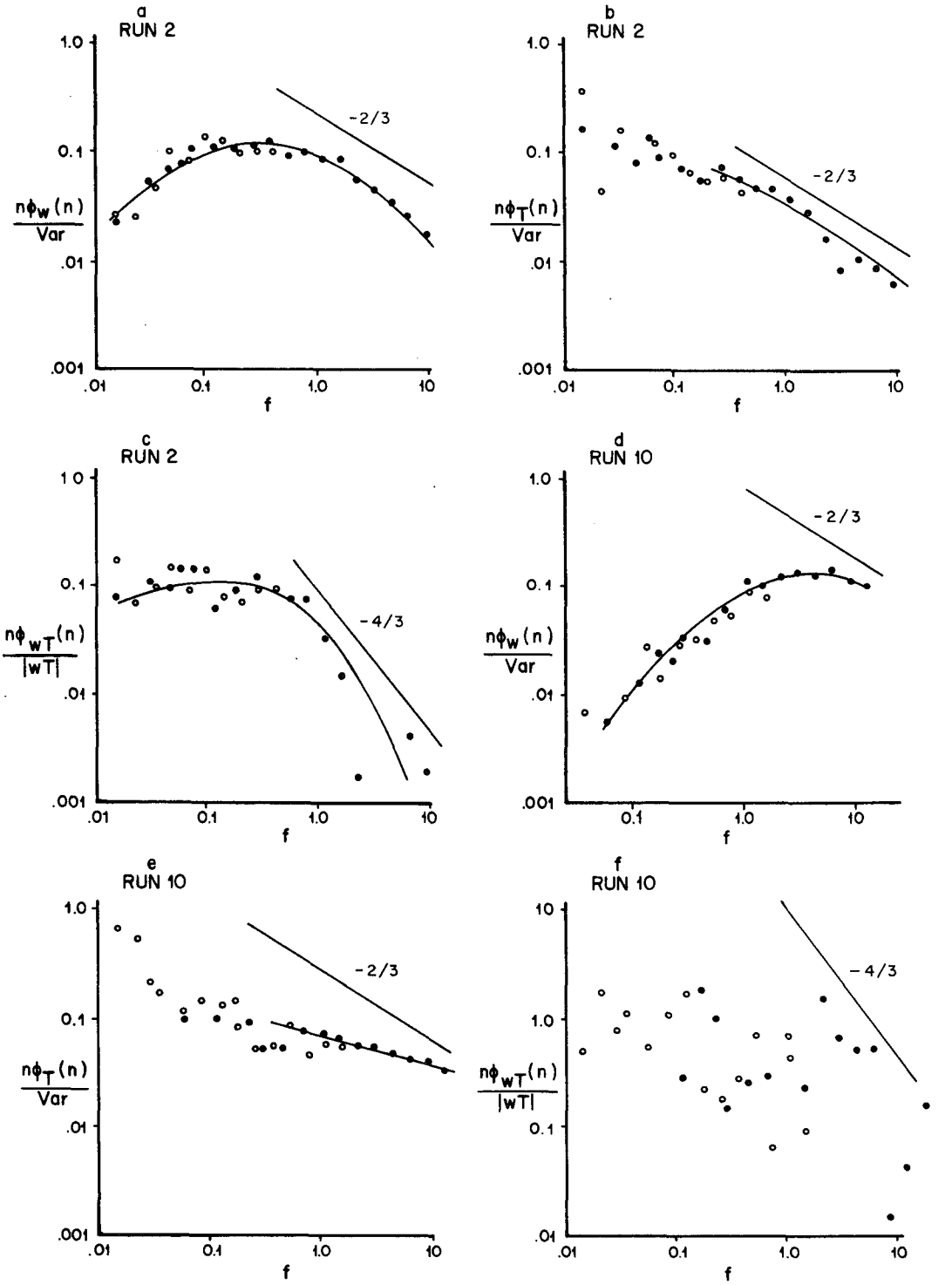

FIG. 4. (a)–(c) Normalized w, T spectra and wT cospectrum for run 2 (unstable). (d)–(f) Normalized w, T spectra and wT cospectrum for run 10 (stable). VAR is the variance of w or T.

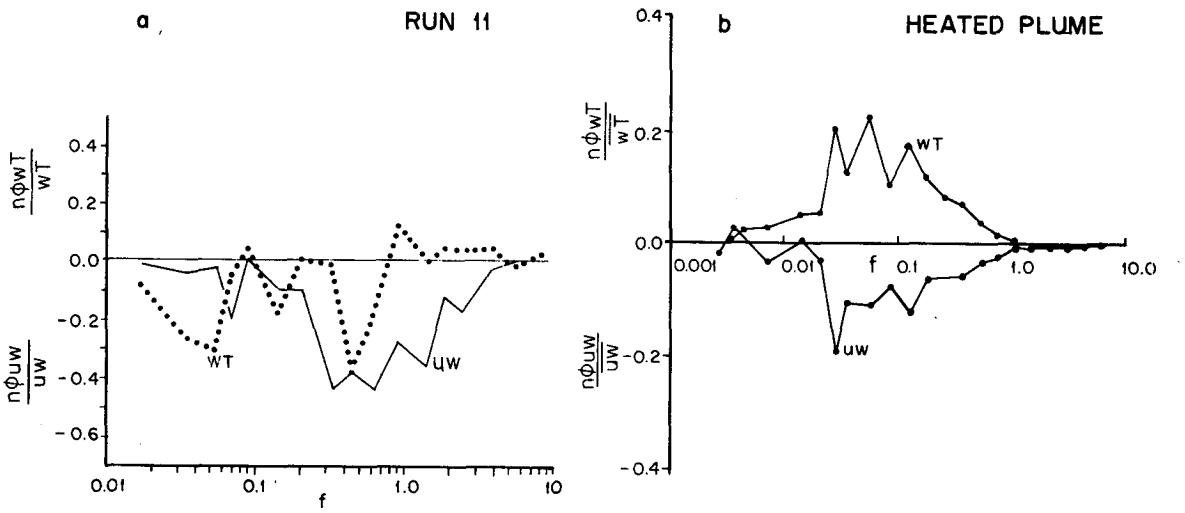

FIG. 5. (a) Normalized heat and momentum fluxes for run 11 (stable). (b) As in Fig. 5a except for heated plume taken over Lake Ontario under stable ambient conditions.

and 6, which represent wind orientations parallel to the road, exhibit strongly accelerated winds at the lower levels of tower 9. At the levels above 8 m the profiles of the two towers tend to become parallel. In the cases of perpendicular flow to the highway (runs 2 and 8), the features are not as pronounced especially with increasing wind speeds. The wind speeds at tower 3 are uniformally higher, probably because of its somewhat higher elevation. Runs 1, 3, 7, 9, 10 and 11, representing wind at oblique angles with respect to the highway, show profile distortions to varying degrees.

c. Impact on near-roadway dispersion

From the comparisons of spectral distributions with and without traffic influence, it appears that significant input of turbulent energy occurs at natural frequencies around 0.25 Hz. The size of traffic-generated eddies—under the assumption of frozen turbulence (Taylor's hypothesis)—is then on the order of 4–8 m (horizontally).

If we follow the general concepts of diffusion expressed by a mean eddy diffusion coefficient multiplied by a concentration gradient, this K (for the vertical component) can be written as (Pasquill, 1974)

$$K_z = C\sigma_w\lambda_m,$$

where C is a constant, σ_w^2 the variance of the vertical wind component and λ_m the wavelength at which maximum spectral power occurs. In reality, of course, K and σ are integral values of all the Fourier components in the spectrum, and λ_m is taken as representative for this spectrum. The shape of the spectrum and hence λ_m are supposed to be dependent on the stability. The stability dependence of K_z, either as a function of the Richardson number or of the Monin-Obukhov stability length L has been extensively treated in the literature. In the case of traffic-generated turbulence, there is an augmentation of turbulent energy at wavelengths well below λ_m. These turbulent eddies will be important for the near-roadway diffusion, but are not properly represented

TABLE 2. Summary of experimental conditions for the wind profile runs. TET and TWT are the total number of vehicles in the eastbound and westbound directions, respectively. Fluct indicates that the wind direction is fluctuating.

Run no.	Date	Run time interval	Wind direction @15 m	Wind direction @2 m	TET	Average speed of the vehicles (km h^{-1})	TWT	Average speed of the vehicles (km h^{-1})
1	6/4/77	1400–1415	320	280	220	80.2	38	78.2
2	6/4/77	0945–1000	350	305	765	29.8	365	89.4
3	6/4/77	1815–1830	305	280	568	79.4	427	91.4
4	6/4/77	2330–2345	265	270	510	77.9	200	91.0
5	6/5/77	0100–0115	265	270	323	76.3	90	86.6
6	6/5/77	1115–1130	280	280	910	77.3	572	91.9
7	6/5/77	1315–1330	305	280	683	79.2	596	92.6
8	6/5/77	1600–1615	350	330	601	81.0	674	92.9
9	6/5/77	2045–2100	30	Fluct	606	77.9	616	91.8
10	6/5/77	2300–2315	30	Fluct	403	79.7	574	93.1
11	6/6/77	1000–1015	75	Fluct	550	75.7	401	90.2

in K_z. Therefore, for purposes of near-roadway dispersion a representation has to be sought, in which K is modified as K_z (total) $= K_z + \Delta K$, where ΔK is a decreasing function of height and downwind distance from the source.

ΔK at a given downwind distance from the source can be estimated from $\Delta K = C_n \Delta\sigma_w \lambda_n$, where ΔK is the contribution from the locally generated turbulence, to K, $\Delta\sigma_w^2$ is the increment of variance in the spectral range for which λ_n is the representative "eddy size";

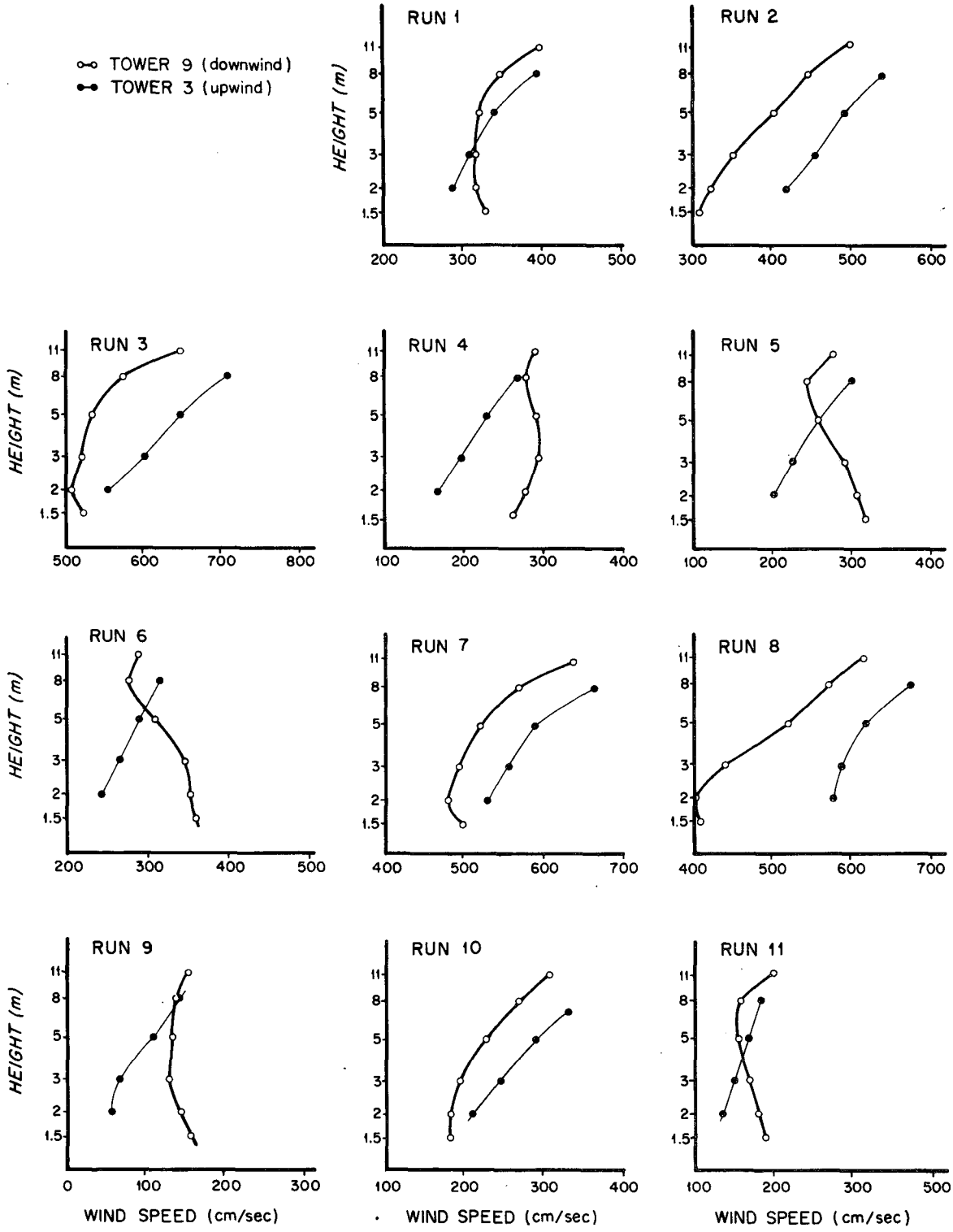

FIG. 6. Observed wind profiles for the various runs in Table 2.

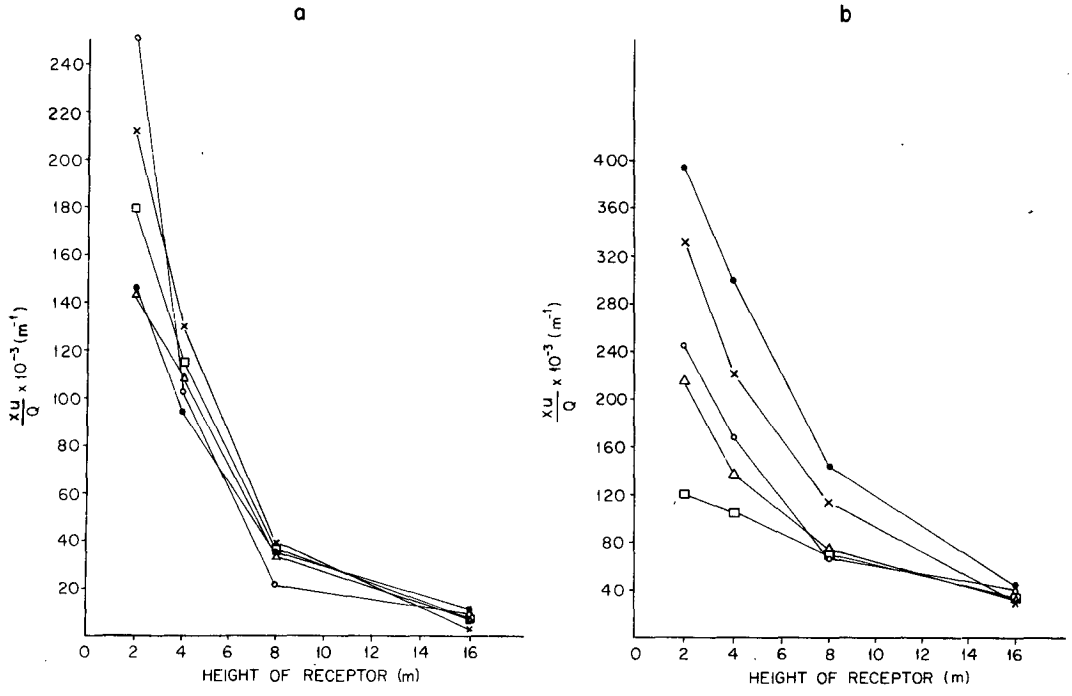

FIG. 7. (a) Normalized concentrations versus receptor height in various tracer gas experiments for perpendicular wind flow to the highway. (b) As in Fig. 7a except for parallel wind flow to the highway.

C_n is the corresponding constant. Calculations of ΔK at a distance of 10 m from the center of the highway indicate that ΔK contribution to the total diffusivity in the unstable cases is about 3–4% of K_z while the ΔK contribution is about 40–100% in the stable case. Consequently, there will be a maximum (X_{max}) distance downwind from the roadway up to which both atmospheric stability (natural turbulence) and traffic (locally generated turbulence) will govern the pollutant dispersion. For distances greater than X_{max}, only atmospheric stability will determine the diffusion process.

A second mechanism that will severely affect the dispersion process, close to the highway, is the aerodynamic drag due to the moving vehicles. The fact that wind profiles are distorted mainly if the wind has a component parallel to the highway means that there is an altered dispersion in the direction of the road.

Fig. 7 shows the normalized concentrations of the tracer gas (sulfur hexafluoride, SF_6) observed close to the highway (~1.5 m from the road edge) as a function of height over the highway in the case of perpendicular (Fig. 7a) and parallel wind-road (Fig. 7b) orientations. Details of the tracer gas release experiments can be found in Rao *et al.* (1978b). It is interesting to see that while there is a considerable variation in the magnitude of the concentrations at lower levels for both parallel and perpendicular wind conditions, the concentrations tend to merge by 8 m in the perpendicular case. In the parallel condition, however, there is still a large variation at 8 m height. It should be pointed out here that, since all the tracer experiments were performed during neutral atmospheric conditions, the variation in the magnitude of the normalized concentrations cannot be attributed to the atmospheric stability. From the observed wind profiles, it is evident that these variations in concentration are due to the wakes behind the moving vehicles.

4. Summary

Several pieces of evidence are combined to draw the following conclusions:

1) With significant moving traffic, there is a noticeable augmentation of turbulent kinetic energy. This turbulent energy appears to be dominant at mean frequencies of 0.1–1.0 Hz corresponding to eddy sizes of a few meters, and is probably due to multiple wakes generated by the moving vehicles.

2) As revealed from a comparison of mean wind profiles close to the highway and at 37 m distance from the highway, the aerodynamic drag due to the moving vehicles is significant. These effects are manifested by an acceleration of wind in the lowest 8 m in cases of wind directions nearly parallel to the highway.

3) In contrast to the findings of Dabberdt (1976) and Chock (1977), no organized convection can be

distinguished in the spectral structure, even under quite stable atmospheric conditions.

Acknowledgments. The authors wish to thank Marsden Chen and Michael Keenan for their help in setting up the experiment. The authors are grateful to Robert Eskridge, William Petersen and Bruce Turner of the Meteorology Laboratory, EPA, for their helpful comments on the manuscript. Thanks are extended to Nancy Gardner and Catherine Cassidy for typing the manuscript and Carol Clas for drafting the diagrams. This research was supported by the United States Environmental Protection Agency under Grant R-804579-01.

REFERENCES

Bradley, E. F., 1968: A micrometeorological study of velocity profiles and surface drag in the region modified by a change in surface roughness. *Quart. J. Roy. Meteor. Soc.*, **94**, 361–379.

Busch, N. E., and H. A. Panofsky, 1968: Recent spectra of atmospheric turbulence. *Quart. J. Roy. Meteor. Soc.*, **94**, 132–148.

Byutner, E. K., 1974: Interaction of a turbulent flow with a surface covered with moving obstacles. *Izv. Atmos. Ocean. Phys.*, **10**, 486.

Chock, D. P., 1977: General Motors sulfate dispersion experiment—An overview of the wind, temperature, and concentration fields. *Atmos. Environ.*, **11**, 553–559.

Czapski, U., and W. G. Mumford, 1975: Heat transfer from a thermal effluent. ASME Publ. 75-HT-24.

Dabberdt, W. F., 1976: Experimental studies of near-roadway dispersion. *Proc. 69th Annual Meeting, Air Pollution Control Ass'n.*, Portland.

Fichtl, G. H., and G. E. McVehil, 1970: Longitudinal and lateral spectra of turbulence in the atmospheric boundary layer at Kennedy Space Center. *J. Appl. Meteor.*, **9**, 51–63.

Haung, C. H., and E. C. Nickerson, 1974a: Stratified flow over non-uniform surface conditions: Mixing-length model. *Bound.-Layer Meteor.*, **5**, 395–417.

——, and ——, 1974b: Stratified flow over non-uniform surfaces: Turbulent energy model. *Bound.-Layer Meteor.*, **7**, 107–123.

Hyson, P., J. R. Garratt and R. J. Francey, 1977: Algebraic and electronic corrections of measured $\overline{uw}$ covariance in the lower atmosphere. *J. Appl. Meteor.*, **16**, 43–47.

Jackson, N. A., 1976: The propagation of modified flow downstream of a change in roughness. *Quart. J. Roy. Meteor. Soc.*, **102**, 924–933.

Japan–U.S. Joint Study Group, 1971: Development of sonic anemometer and its application to the study of atmospheric surface layers. *Disaster Prev. Res. Inst., Kyoto, Japan*, No. 6. 250 pp.

Kaimal, J. C., J. C. Wyngaard and D. A. Haugen, 1968: Derived power spectra from a three-component sonic anemometer. *J. Appl. Meteor.*, **7**, 827–836.

——, ——, Y. Isumi and O. R. Cote, 1972: Spectral characteristics of surface layer turbulence. *Quart. J. Roy. Meteor. Soc.*, **98**, 563–589.

Lo, A. K., 1977: Boundary layer flow over gentle culvilinear topography with a sudden change in surface roughness. *Quart. J. Roy. Meteor. Soc.*, **103**, 199–209.

Munro, D. S., and T. R. Oke, 1975: Aerodynamic boundary layer adjustment over a crop in neutral stability. *Bound.-Layer Meteor.*, **9**, 53–61.

Pasquill, F., 1974: *Atmospheric Diffusion*, 2nd ed. Wiley, 429 pp.

Peterson, E. W., L. Kristensen and C. C. Su, 1976: Some observations and analysis of wind over non-uniform terrain. *Quart. J. Roy. Meteor. Soc.*, **102**, 857–869.

Rao, S. T., and C. B. Ketchum, 1975: Spectral characteristics of baroclinic annulus waves. *J. Atmos. Sci.*, **32**, 698–711.

——, M. Chen, M. T. Keenan, G. Sistla, P. J. Samson and D. Romano, 1978a: Overview of the NYS-Long Island expressway dispersion experiment. *Proc. 57th Annual Meeting of the Transportation Research Board*, Session 25, National Research Council, Washington, DC.

——, ——, ——, ——, R. Peddada, G. Wotzak and N. Kolak, 1978b: Dispersion of pollutants near highways: Experimental design and data acquisition procedures. EPA-600-4-78-037, 55 pp.

Stearns, C. R., and H. H. Lettau, 1963: Report on two wind-profile modification experiments in airflow over the ice of Lake Mendota. Annual Report, Dept. of Meteorology, University of Wisconsin, 115–138.